JOURNAL OF MOLECULAR SPECTROSCOPY 81, 316–326 (1980)

Tunable Laser Study of the $\nu_{10} + \nu_{11}$ Band of Cyclopropane

W. H. WEBER

Research Staff, Ford Motor Co., Dearborn, Michigan 48121 and Physics Department, University of Michigan, Ann Arbor, Michigan 48109

D. H. LESLIE[1] AND C. W. PETERS

Physics Department, University of Michigan, Ann Arbor, Michigan 48109

AND

R. W. TERHUNE

Research Staff, Ford Motor Co., Dearborn, Michigan 48121

Diode laser measurements of the $\nu_{10} + \nu_{11}$ ($l_{tot} = \pm 2$) perpendicular band of cyclopropane have led to the assignments of roughly 600 lines in the 1880–1920-cm^{-1} region. Most of the spectra were recorded and stored in digital form using a rapid-scan mode of operating the laser. These spectra were calibrated, with the aid of a computer, by reference to the R lines of the $\nu_1 + \nu_2$ band of N_2O. The ground state constants we obtained are (in cm^{-1}) $B = 0.670240 \pm 2.4 \times 10^{-5}$, $D_J = (1.090 \pm 0.054) \times 10^{-6}$, $D_{JK} = (-1.29 \pm 0.19) \times 10^{-6}$, $D_K = (0.2 \pm 1.1) \times 10^{-6}$. The excited state levels are perturbed at large J values, presumably by Coriolis couplings between the active $E'(l_{tot} = \pm 2)$ and the inactive $A'(l_{tot} = 0)$ states. Effective values for the excited state constants were obtained by considering only the $J < 15$ levels. The A_1–A_2 splittings in the $K' = 1$ excited states were observed to vary as $q_{eff}J(J + 1)$, with $q_{eff} = (2.17 \pm 0.17) \times 10^{-4}$ cm^{-1}.

I. INTRODUCTION

We describe a high resolution study of the $\nu_{10} + \nu_{11}$ perpendicular band of C_3H_6 cyclopropane using tunable diode lasers. Since cyclopropane has no permanent dipole moment, no rotational microwave transitions are allowed and the determination of its molecular constants must come from either ir vibration-rotation spectra or Raman spectra measurements. The most accurate values for the ground state constants have been obtained from an analysis of the infrared ν_6 parallel band at 3100 cm^{-1} by McCubbin *et al.* (*1*), and, very recently, from a pure rotational Raman study by Rubin *et al.* (*2*). There have been several moderate resolution studies of the rotational structure of infrared bands, but the only previous fully resolved analysis of a perpendicular band of C_3H_6 was that by Maki (*3*) of $\nu_5 + \nu_{10}$. Butcher and Jones (*4*) have analyzed rotational structure in several perpendicular Raman bands and have obtained the most accurate value for the C rotational constant. Cartwright and Mills (*5*) showed through analyses of moder-

[1] Present address: Science Applications Inc., 15 Research Drive, Ann Arbor, MI 48103.

0022-2852/80/060316-11$02.00/0

ate resolution band contours that strong *l*-resonance perturbations occur in many of the perpendicular vibration fundamentals of C_3H_6. Their conclusions were verified by Maki's high resolution work. Duncan (*6*) studied several of the infrared bands of C_3H_6, including the $\nu_{10} + \nu_{11}$ band discussed here, and Duncan and Burns (*7*) reported the force field and normal coordinates of cyclopropane-H_6 and -D_6.

The next section of this paper describes the experimental details. Doppler resolution limited, tunable diode laser spectra were used for all the analysis reported here, and these spectra were calibrated against the N_2O spectrum recently reported by Amiot and Guelachvili (*8*). The third section describes our procedure for making assignments and analyzing the data. The resulting ground state constants B_0, D_J, and D_{JK} are in good agreement with those of Rubin *et al.* In the fourth section we discuss the fitting of the excited state. The $\nu_{10} + \nu_{11}$ vibrational state is a combination of two doubly degenerate E' fundamentals and the resultant state can have species A_1', A_2', and E' of the D_{3h} point group. Although only the transition to the E' state of $\nu_{10} + \nu_{11}$ is infrared active, the Coriolis interactions can mix the A and E components, resulting in sizeable perturbations of levels with large J values. Accordingly we have restricted our fitting of the excited state to $J < 15$ levels and have used an energy expression appropriate to a singly excited E' vibration with "effective" ζ and η interaction constants.

II. EXPERIMENTAL DETAILS

The diode laser spectra were obtained using two PbSSe diode lasers—one from A. D. Little, Inc., which covered the region 1880–1900 cm^{-1}, and one from Laser Analytics, Inc., which covered the region 1895–1960 cm^{-1}. The lasers were mounted on the copper cold finger of an Air Products, Inc., Heli-Tran Liquid Helium Transfer Refrigerator. The refrigerator attained an ultimate temperature of 7 K. The emission frequency of the diode laser varies with its temperature. In order to coarsely tune the output frequency, this temperature could be raised by reducing the He flow and by dissipating electric power in a small resistance heater on the cold finger. To obtain a stable temperature in the 20–30-K range it was generally necessary both to use the heater and adjust the He flow. All spectral scans with the lasers were done by sweeping the dc current used to pump the laser while the heater power and He flow were held constant. Isolated C_3H_6 lines at pressures below 1 Torr exhibited a full-width at half-absorption strength within a few percent of the predicted Doppler width, 0.0036 cm^{-1}, indicating that the laser linewidth is substantially narrower.

We were able to exert some control over the relative strengths of the modes of the A. D. Little laser by using a small electromagnet ($B \cong 10$ kG) oriented with the field perpendicular to the p–n junction plane of the diode. This control amounted to extending the tuning ranges of some of the modes by as much as one wavenumber. The magnet had no significant effect on the Laser Analytics laser.

The optical setup, shown in Fig. 1, involved a double-beam arrangement similar to that described previously (*9*). A 25-cm focal length Jarrel–Ash spectrometer was used to select individual laser modes. The spectrometer was normally used with 100-μm slits and with a 100-lines/mm grating, giving a linear

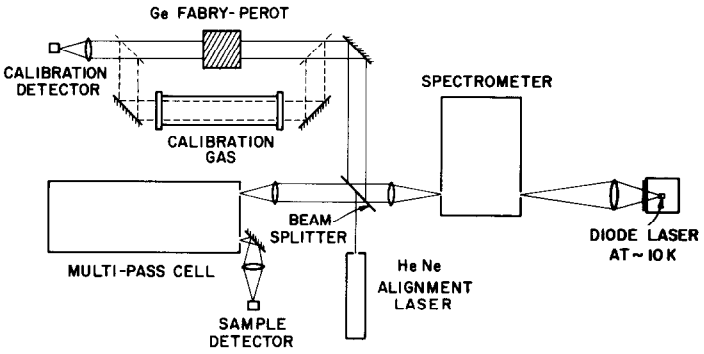

FIG. 1. Schematic drawing of optical setup used to obtain diode laser spectra.

dispersion of 10^{-2} cm per wave number. The beam splitter was a ZnSe flat AR coated on one surface. The same beam splitter was used to introduce a HeNe laser beam into the optical paths for alignment. The sample beam passed through a Wilks variable path absorption cell with a maximum pathlength of 20 m, and was focused onto a HgCdTe detector. The calibration beam passed through either a Fabry–Perot etalon or a 50-cm cell containing a calibration gas before being focused onto a PbTe photovoltaic detector. Both detectors operated at 77 K. The calibration beam could be quickly switched from the etalon to the gas cell by moving two small mirrors on rotatable mounts.

Relative frequencies were measured by reference to the interference fringes from a 3.7879-cm thick uncoated Ge etalon. The free spectral range of the etalon, calculated from the known refractive index (*10*), was 0.032661 cm^{-1} at 1880 cm^{-1} and 0.032646 cm^{-1} at 1920 cm^{-1}. Since temperature changes of the etalon during a scan can lead to large calibration errors, the etalon was mounted in a large Cu block to increase its thermal mass; the block was then mounted in a large styrofoam cylinder to isolate it from changes in room temperature. The styrofoam cylinder and Cu block had small holes in each end to allow the beam to pass through.

Absolute calibration was done by reference to the $R(J)$ lines of the $\nu_1 + \nu_2$ band of $^{14}N_2{}^{16}O$. These lines have recently been measured by Amiot and Guelachvili (*8*) with an internal consistency of $\pm 1 \times 10^{-4}$ cm^{-1}. They are particularly convenient for calibration, being spaced roughly 0.7 cm^{-1} apart and spanning the full region of the C_3H_6 band under study. We were also able to use the N_2O lines to verify that the etalon calibration is accurate to at least one part in 3000.

Two quite different scanning modes were used to record the spectra. In the slow-scan mode, which was used for most of the spectra below 1895 cm^{-1}, the laser frequency is slowly swept at a rate of $\cong 5 \times 10^{-3}$ cm^{-1}/sec, a mechanical chopper at the entrance slit chops the beam at $\cong$400 Hz, two lock-in amplifiers measure the intensities in the sample and calibration beams, and the signals from the lock-in amplifiers are recorded with a two-pen chart recorder. Each sample spectrum is recorded twice, once each with either the etalon or the N_2O cell

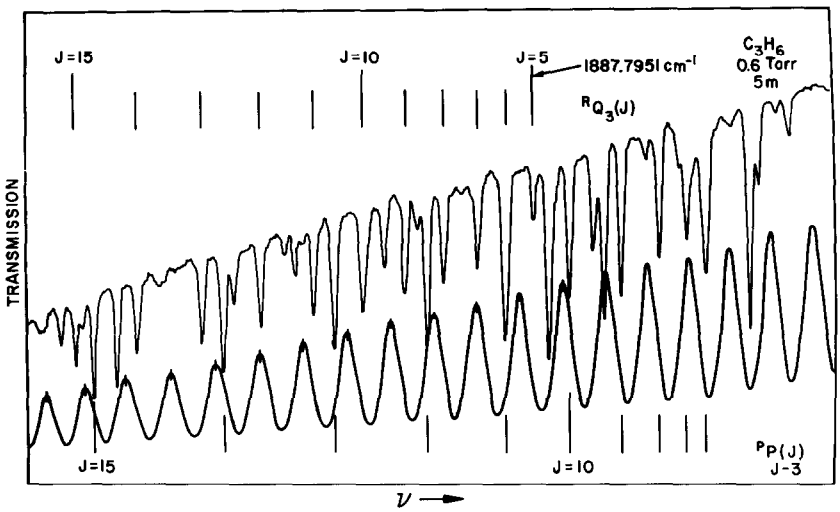

FIG. 2. Diode laser spectrum of C_3H_6 obtained in the slow-scan mode. The sample and etalon scans were recorded simultaneously and the zero transmission level is at the bottom of the graph for both traces. The fringe spacing is 0.032658 cm^{-1}.

in the calibration beam. From these records, using a ruler and a calibrated eyepiece, the frequencies of isolated C_3H_6 lines could be measured relative to the N_2O lines with an accuracy of $\pm 2 - 10 \times 10^{-4}$ cm^{-1}. Aside from blending of the C_3H_6 lines, locating the centers of the N_2O lines was the primary limitation on the accuracy. The N_2O band is a weak combination band and we did not have access to a second multipass cell for the N_2O sample. An example of the spectra obtained in the slow-scan mode is shown in Fig. 2.

A fast-scan mode was implemented during the later stages of this research, and it was used for the spectra above 1895 cm^{-1}. In this mode the laser frequency is swept repetitively over about a 1-cm^{-1} region at a rate of 20 cm^{-1}/sec. There is no mechanical chopper in the beam. The amplified outputs of the two detectors can be viewed directly on an oscilloscope. The bandpass of the sample-beam detector extends from roughly 10 Hz to 1 MHz. The low-frequency cutoff removes the change in the baseline produced by the slow change in the laser signal from one part of the scan to another. The high frequency cutoff is sufficient to give an accurate reproduction of the true Doppler-broadened lineshape. The spectra appear as sharp lines on a rather flat baseline. One disadvantage of this scanning mode is that there is no accurate baseline to establish the absolute intensity of a given line. The relative strengths of nearby lines are reproduced well, but those of widely separated lines are not. This disadvantage is greatly outweighed by the advantage of being able to view and select the spectra in real time before recording them.

A Model NS-575A Tracor Northern digital signal averager was used to record the data in the fast-scan mode. Typically 100–200 scans were averaged to improve the signal-to-noise ratio. The averaged spectra were then stored as 4096 point digital records on magnetic tape. Three spectra were recorded sequentially, one each of the sample gas, the calibration gas, and the Fabry-Perot fringes. These spectra

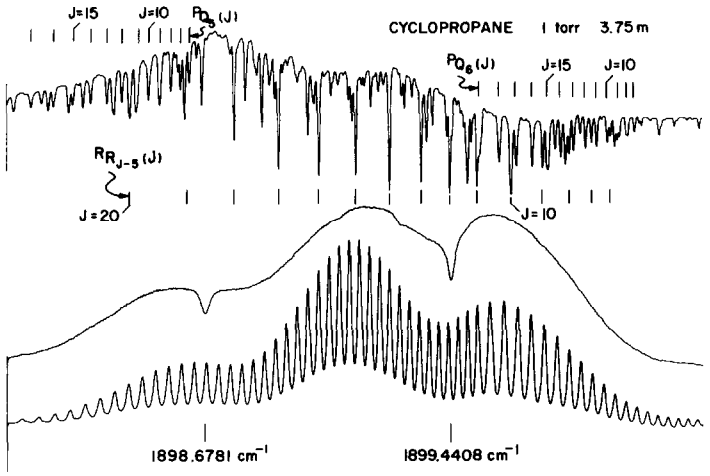

FIG. 3. The top trace is a diode laser spectrum of C_3H_6 taken in the rapid-scan mode described in the text. The absolute calibration lines, shown on the middle trace, are the $R(22)$ and $R(23)$ 11^10-00^00 N_2O lines at 1898.6781 cm^{-1} and 1899.4408 cm^{-1}, respectively. The bottom trace gives the relative frequency calibration with a fringe spacing of 0.032654 cm^{-1}. The slow modulation apparent in all three scans is caused by interference in the beam splitter.

have a common frequency scale. The total time needed to record them was less than one minute. An example of the three spectra is shown in Fig. 3. Analysis of the spectra was then done on a DEC 10 computer using Fortran programs, and the result was a printout of absolute line frequencies and relative strengths. This computerized data analysis system was both faster and more accurate than the methods used for analyzing the slow-scan data.

The use of a double-beam system with the Fabry-Perot after the spectrometer leads to a small but systematic change in the apparent free spectral range due to the motion of the image at the exit slit (*11*). This effect, which amounts to a correction of $\cong 1 \times 10^{-4}$ cm^{-1} at the extremities of a scan, was included in our calibration program.

III. ASSIGNMENTS AND GROUND STATE CONSTANTS

The rotational energy of an oblate symmetric top in its ground vibrational state is given by (*12*)

$$F''(J,K) = B''[J(J+1) - K^2] + C''K^2 - D''_J J^2(J+1)^2 - D''_{JK}K^2J(J+1) - D''_K K^4, \quad (1)$$

where B'' and C'' are the rotational constants; D''_J, D''_{JK}, and D''_K are the centrifugal distortion constants; J is the total angular momentum quantum number; and K is the quantum number assigned to the projection of **J** along the symmetry axis. A similar formula, modified for the effects of vibrational angular momentum, gives the rovibrational energy in an E' degenerate vibrational state (*12*)

$$F'(J,K) = \nu_0 + B'[J(J+1) - K^2] + C'K^2 - 2C'\zeta_r K - D'_J J^2(J+1)^2 - D'_{JK}K^2J(J+1) - D'_K K^4 + \eta^J_r KJ(J+1) + \eta^K_r K^3, \quad (2)$$

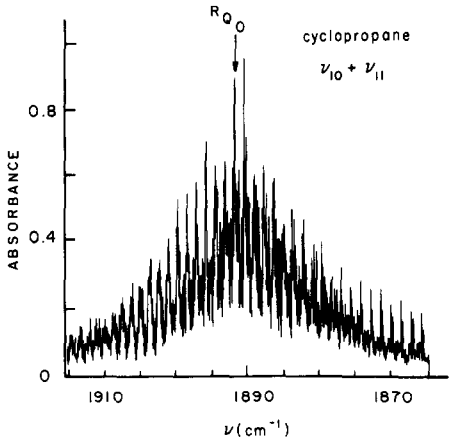

FIG. 4. Fourier transform spectrum of the $\nu_{10} + \nu_{11}$ band of C_3H_6. Experimental conditions: 0.05 Torr, 40-m path, 0.05-cm^{-1} resolution.

where ζ_v is the first order Coriolis splitting parameter given by a sum over the degenerate vibrations v_i which are excited,

$$\zeta_v = \sum_i \zeta_i l_i; \tag{3}$$

the η terms are centrifugal distortion corrections to ζ_v given by similar sums over the degenerate vibrations,

$$\eta_v^J = \sum_i \eta_i^J l_i, \qquad \eta_v^K = \sum_i \eta_i^K l_i; \tag{4}$$

and $l_i\hbar$ is the vibrational angular momentum of the ith degenerate vibration. In the $\nu_{10}(E') + \nu_{11}(E')$ state of symmetry E', we must have $l_{10} = l_{11} = \pm 1$, thus $l_{\text{tot}} = \sum l_i = \pm 2$. If we choose K in Eq. (2) to be a signed quantity, with K positive for those transitions with $\Delta K = +1$, $(+l)$ transitions, and negative for $\Delta K = -1$, $(-l)$ transitions, then we must choose $l_{10} = l_{11} = -1$ (*13*).

Figure 4 shows a Fourier transform spectrum of the $\nu_{10} + \nu_{11}$ band of C_3H_6. In a perpendicular band of a symmetric top molecule the $^RQ_0$ branch should be located near the center of the band with the remaining Q branches spaced roughly $2[C'(1 - \zeta_v) - B']$ spreading out to either side of the center. From previous measurements (*4*, *5*) $\zeta_{10} = -0.076$ and $\zeta_{11} = -0.96$, thus ζ_v is expected to be approximately 1.036. This leads to a value of $\cong -1.36$ cm^{-1} for the Q branch spacing, indicating that the ^RQ branches are below the band center and the ^PQ branches above. Because of the statistical weights in C_3H_6, there should be an intensity alternation of 6:5:5 in the $^{P,R}Q_K$ branches, the higher intensity being associated with those Ks which are a multiple of 3 (*14*). On the basis of these considerations, Duncan (*6*) correctly assigned the Q branches in this band, beginning with the $^RQ_0$ branch at 1891.9 cm^{-1}. There is some indication of the intensity alternation consistent with this assignment on the high frequency side of the spectrum in Fig. 4, but it is not very convincing. The lack of an obvious intensity alternation arises from the fact that $2B = 1.34$ cm^{-1} is very nearly equal in magnitude to $2[C'(1 - \zeta_v) - B']$, the Q-branch spacing. In this case each Q-branch becomes overlapped by

clusters of ${}^{P}P$ or ${}^{R}R$ lines: the ${}^{R}Q_K$ branches by the ${}^{P}P_{J-K}(J)$ lines and the ${}^{P}Q_K$ branches by the ${}^{R}R_{J-K+1}(J)$ lines. Examples of this overlapping are evident in Figs. 2 and 3. These clusters of ${}^{R}R$ and ${}^{P}P$ lines form series with spacings similar to those found in the Q branches. These lines are generally twice as strong as the neighboring Q-branch lines and dominate the apparent intensity under low resolution.

The statistical weights in C_3H_6 also lead to a 2:1 intensity alternation between odd and even Js in the ${}^{R}Q_0$ branch, a feature which should stand out at high resolution. Unfortunately, the ${}^{R}Q_0$ branch is so strongly overlapped by the ${}^{P}P_J(J)$ lines that this intensity alternation cannot be easily recognized. The sharp peak absorption near the center of the band is, in fact, due more to the ${}^{P}P_J(J)$ lines than the ${}^{R}Q_0$ lines.

In order to make any firm assignments, we resorted to ground state combination differences of the form

$$\begin{aligned}\Delta''(J,K) &= \{{}^{R}R_K(J-1) - {}^{R}Q_K(J)\}/2J \\ &= \{{}^{P}Q_K(J-1) - {}^{P}P_K(J)\}/2J \\ &= B'' - D''_{JK}K^2 - 2D''_J J^2, \end{aligned} \tag{5}$$

where, at the outset, we let $D''_{JK} = 0$ and used the previous values of McCubbin *et al.* (*1*) for B'' and D''_J. Once clusters of ${}^{R}R$, ${}^{P}P$, and ${}^{R,P}Q$ lines had been identified, the J values could be assigned by matching pairs of lines to the calculated combination differences. The K value then could be assigned by the 6:5:5 intensity variation in each ${}^{R}R$ or ${}^{P}P$ series, which could always be seen at high J where overlapping was not a problem. The 2:1 intensity alternation between the odd- and even-J ${}^{R}R_0(J)$ lines was also apparent.

The observed relative intensities of the ${}^{R}R$, ${}^{P}P$, and Q branch lines are in agreement with the predicted values (*15*). The ${}^{P}R$ and ${}^{R}P$ lines are calculated to be substantially weaker than the other lines, and only a few of them were assigned. Roughly 10% of the total number of moderate to strong intensity lines still remain unassigned. These fall mostly in the 1885–1895-cm^{-1} region.

Over 100 combination differences $\Delta(J,K)$ were measured. The maximum K value was 17 and the maximum J was 22. These differences were then used in a linear, weighted least-squares fit to Eq. (5) to determine the coefficients B'', D''_{JK}, and D''_J. The data points were weighted inversely as the square of $\sigma_{J,K}$, the estimated uncertainty of $\Delta''(J,K)$, the values of which ranged from 0.7 to 3.0×10^{-4} cm^{-1}. The results are summarized in Table I. The reduced χ^2 statistic, which has an expected value of 1 if the random errors have been properly estimated, was found to be 0.32. This indicates that we have overestimated the statistical errors and that the 1σ uncertainties quoted are conservative estimates. Our uncertainty on the B value is somewhat better than that obtained by Rubin *et al.* (*2*) but the uncertainties on the Ds are comparable, since they were able to use much higher J and K values.

Note that the combination difference relation (5) assumes that the A_1–A_2 splittings in the excited states are unresolved. This was indeed found to be the case except for the $K = 1$ excited state. Thus, no transitions of the type ${}^{R}R_0$ or ${}^{R}Q_0$ could be used in the ground state fit.

TABLE I

Ground State Constants in cm^{-1} Units for Cyclopropane

B	$D_J \times 10^6$	$D_{JK} \times 10^6$	Ref.
0.67024 ±0.00015	0.82 ±0.15	$\|D_{JK}\| < 1.5$	1
0.67028 ±0.00015	1.00 ±0.09	-1.3 ±0.4	2
0.670240±0.000024	1.090±0.054	-1.29±0.19	Present Work

IV. EXCITED STATE

Our starting point for the determination of the excited state constants is Eq. (2). By including *l*-resonance Maki (*3*) was able to adequately fit the $\nu_5 + \nu_{10}$ state through K and $J = 31$ using an energy expression similar to Eq. (2), but without the η terms. The *l*-resonance effects are straightforward when one quantum of an E' vibration is excited, since the states differing by $\Delta K = \pm 2$, $\Delta l_{tot} = \pm 2$ are coupled in pairs by a $q_t^{(+)}$ type interaction. A closed-form expression involving the exact solution to a 2×2 determinant then gives the resulting energies (*5*).

TABLE II

Results of Least-Squares Fit to the $\nu_{10} + \nu_{11}$, E' State of Cyclopropane*

ν_o	=	1893.0551±0.0010	
B'	=	$0.668\ 698 \pm 1.3 \times 10^{-5}$	
C'	=	$0.413\ 897 \pm 3.4 \times 10^{-5}$	a
$C'\zeta_v$	=	$0.426\ 631 \pm 6.8 \times 10^{-5}$	b
D'_J	=	$(1.026 \pm 0.084) \times 10^{-6}$	
D'_{JK}	=	$-(0.27 \pm 0.20) \times 10^{-6}$	
D_K	=	$(0.17 \pm 1.08) \times 10^{-6}$	c
η_v^J	=	$-(1.95 \pm 0.10) \times 10^{-5}$	
η_v^K	=	$(7.47 \pm 0.46) \times 10^{-5}$	
q_{eff}	=	$(2.17 \pm 0.17) \times 10^{-4}$	

[a] The value of C" was constrained to be 0.4177 cm^{-1} (4). Since our data are primarily sensitive to C'-C", a shift in C" would give a similar shift in C'.

[b] This value yields $\zeta_v = 1.0308 \pm 0.0003$.

[c] D'_K and D''_K were constrained to be equal.

* The ground state constants were constrained at the values given in Table I. The maximum J and K was 14 and the rms error of the fit was 0.0028 cm^{-1} for 271 lines. Values are in cm^{-1}. The uncertainties are 2σ estimates.

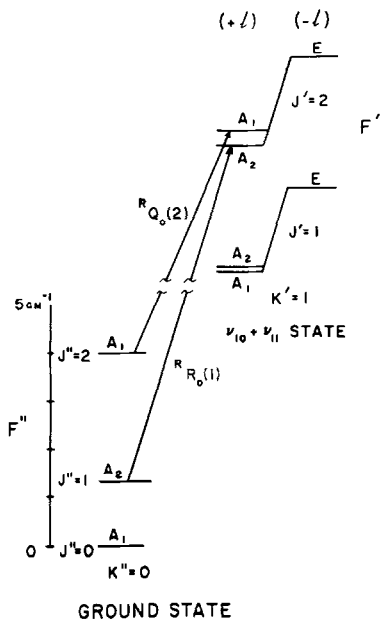

FIG. 5. Energy level diagram showing the transitions used to determine the A_1–A_2 splittings in the $\nu_{10} + \nu_{11}$, $K' = 1$ state. The rotational spacings are drawn roughly to scale, but the A_1–A_2 splittings have been exaggerated for clarity.

When two different E' vibrations are simultaneously excited, the resultant vibrational state can have species $A_1'(l_{tot} = 0)$, $A_2'(l_{tot} = 0)$, or $E'(l_{tot} = 2)$. Only the E' species is infrared active and, since the condition for l-resonance, $\zeta_{t'} \cong -0.6$, is not satisfied in $\nu_{10} + \nu_{11}$, we might expect the energy expression (2) to be adequate. Unfortunately, for J greater than 14–15 the energy levels begin to show marked deviations from Eq. (2). This was first indicated by the excited state combination differences, ${}^RR(J) - {}^RQ(J)$ and ${}^PP(J) - {}^PQ(J)$. To obtain the excited state constants we therefore restricted $J < 15$. We also constrained $D_K' = D_K''$, since no significant difference between these constants could be determined. Our results are summarized in Table II. The lines were assigned an uncertainty of ± 0.0020 cm^{-1} and were equally weighted in the fit. The quoted errors are 2σ estimates, with no allowance made for the uncertainties in the ground state constants.

The deviations from Eq. (2) observed for high-J values occur for all J and K and are definitely not local resonances. Very likely they are caused by l-type couplings between the A and E component vibrations. Amat *et al.* (*16*) have considered the effects of such couplings using second-order perturbation theory. We have not attempted to include these effects in the excited state energy levels. To do so would require the introduction of several additional new parameters, and without some a priori knowledge of the positions of the A levels the problem appears to be very complex.

We have been able to observe one effect of l-type coupling in the excited state, namely, the A_1–A_2 splitting in the $K = 1$ manifold, which is referred to by Amat *et al.* as the $Kl_t = -1$ splitting. Such a splitting has been reported recently in the

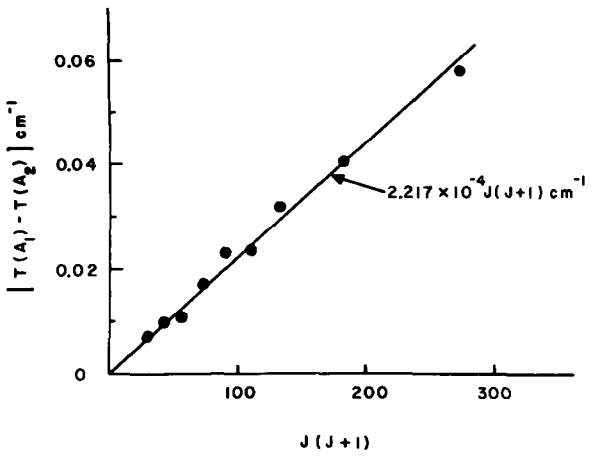

FIG. 6. Experimental determination of the A_1–A_2 splitting in the $\nu_{10} + \nu_{11}$, $K' = 1$, state of C_3H_6. The data points are obtained from Eq. (6), and the straight line is a least-squares fit constrained to pass through the origin.

microwave spectrum of trioxane (*17*), but we are aware of no previous observation of this splitting in infrared spectra of a symmetric top. The relevant energy level diagram showing the transitions used to measure the splitting is shown in Fig. 5. The A_1 and A_2 levels are directly coupled, leading to an energy separation of the form:

$$T(A_1) - T(A_2) = \pm q_{\text{eff}} J(J + 1),$$

where, following the convention of Cartwright and Mills (*5*), we take the plus sign for J even and the minus for J odd. The A_1–A_2 splitting is given by the difference between the appropriate R- and Q-branch transitions, corrected for the lower level energy differences:

$$^{R}R_0(J - 1) - {}^{R}Q_0(J) - 2B''J + 4D''_J J^3 = q_{\text{eff}} J(J + 1). \tag{6}$$

Figure 6 shows a plot of the combination difference relation yielding the $Kl_t = -1$ splitting. The straight line in Fig. 6 is a least-squares fit constrained to pass through the origin. The slope differs slightly from the value in Table II, since that value was obtained using several additional lines for which we had no combination differences. It is interesting to note that q_{eff} in $\nu_{10} + \nu_{11}$ is roughly an order of magnitude smaller than the corresponding parameters $q_{\text{eff}}(\nu_{10}) = 2.5 \times 10^{-3}\ \text{cm}^{-1}$ and $q_{\text{eff}}(\nu_{11}) = 6.5 \times 10^{-3}\ \text{cm}^{-1}$ found in the fundamentals (*5*).

We have also looked for and not found any evidence for A_1–A_2 splittings in other K manifolds, particularly $K = 2$, which should give the next largest effect. We can conclude from our data that for $J \lesssim 25$ the A_1–A_2 splittings in the $K \neq 1$ manifolds are substantially less than the Doppler broadening.

ACKNOWLEDGMENTS

We are indebted to P. D. Maker, N. Savage, H. Niki, and L. P. Breitenbach for providing the Fourier transform spectra and to B. P. Poindexter for assistance in recording the diode laser spectra.

We wish to thank T. K. McCubbin for sending us a reprint of Ref. (*2*) and also J. M. Colmont for communicating his results on trioxane prior to publication.

RECEIVED: June 4, 1979

REFERENCES

1. T. K. MCCUBBIN, JR., V. WITHSTANDLEY, AND S. R. POLO, *J. Mol. Spectrosc.* **31,** 95–99 (1969).
2. B. RUBIN, D. A. STEINER, T. K. MCCUBBIN, JR., AND S. R. POLO, *J. Mol. Spectrosc.* **72,** 57–61 (1978).
3. A. G. MAKI, *J. Mol. Spectrosc.* **41,** 177–181 (1972).
4. R. J. BUTCHER AND W. J. JONES, *J. Mol. Spectrosc.* **47,** 64–83 (1973).
5. G. J. CARTWRIGHT AND I. M. MILLS, *J. Mol. Spectrosc.* **34,** 415–439 (1970).
6. J. L. DUNCAN, *J. Mol. Spectrosc.* **25,** 451–466 (1968).
7. J. L. DUNCAN AND G. R. BURNS, *J. Mol. Spectrosc.* **30,** 253–265 (1969).
8. C. AMIOT AND G. GUELACHVILI, *J. Mol. Spectrosc.* **59,** 171–190 (1976).
9. W. H. WEBER, P. D. MAKER, AND C. W. PETERS, *J. Chem. Phys.* **64,** 2149–2158 (1976).
10. American Institute of Physics Handbook, (D. E. Gray, Ed.), 3rd ed., Chap. 6, p. 30, McGraw–Hill, New York, 1972.
11. H. FLICKER, J. P. ALDRIDGE, H. FILIP, N. G. NERESON, M. J. REISFELD, AND W. H. WEBER, *Appl. Optics* **17,** 851–852 (1978).
12. I. M. MILLS, *in* "Molecular Spectroscopy: Modern Research" (K. Narahari Rao and C. W. Mathews, Eds.), Vol. 1, pp. 115–140, Academic Press, New York, 1972.
13. D. R. J. BOYD AND H. C. LONGUET-HIGGINS, *Proc. Roy. Soc. London Ser. A* **213,** 55–73 (1952).
14. E. B. WILSON, JR., *J. Chem. Phys.* **3,** 276–285 (1935).
15. G. HERZBERG, "Infrared and Raman Spectra," p. 426, Van Nostrand, New York, 1945.
16. G. AMAT, H. H. NIELSON, AND G. TARRAGO, "Higher Order Rotation-Vibration Energies of Polyatomic Molecules," p. 251, Dekker, New York, 1971.
17. J. M. COLMONT, "Abstracts of 33rd Symposium on Molecular Spectroscopy, Columbus, Ohio, June 12–16, 1978," p. 85; and unpublished results.